

Direct laser cooling to Bose-Einstein condensation in a dipole trap: Supplemental material

Alban Urvoy,* Zachary Vendeiro,* Joshua Ramette, Albert Adiyatullin, and Vladan Vuletić†
*Department of Physics, MIT-Harvard Center for Ultracold Atoms and Research Laboratory of Electronics,
 Massachusetts Institute of Technology, Cambridge, Massachusetts 02139, USA*
 (Dated: April 24, 2019)

OPTICAL PUMPING DETUNING

To find an optical pumping detuning that avoids losses from molecular resonances as predicted in Refs. [S1, S2], we start with a cold cloud of atoms and measure the loss spectrum below threshold (i.e. bare atomic resonance) for light-atom detunings Δ above -18 GHz. This is closer to resonance than previously explored experimentally on the D_1 -line of ^{87}Rb [S3–S5]. After executing a sequence which scatters the same number of photons, about 100, regardless of detuning, we obtain a fraction of surviving atoms as given in Fig. 4(a) of the main text, with frequency regions where the remaining atom number is relatively large shown in Fig. S1. The scan is performed with a resolution of 10 MHz. The optimum around -4.33 GHz in Fig. S1(b) was chosen due to its good performance. Other optima could be used as well, and better optima may exist outside the range of this scan.

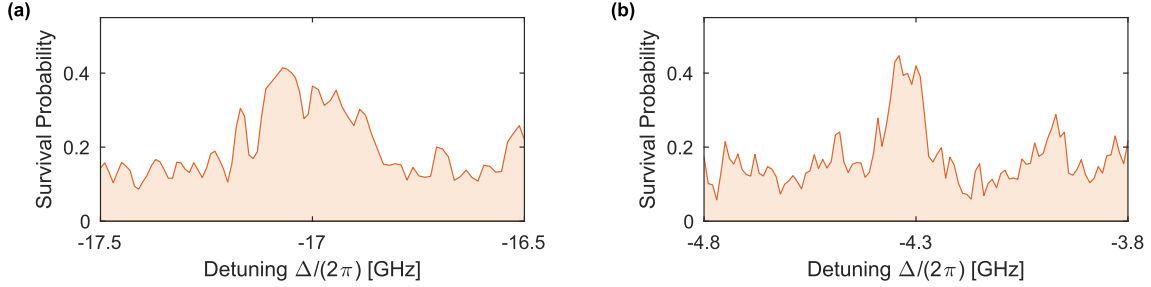


FIG. S1. Survival probability of the atoms in the trap as a function of detuning after repeated cycles of optical pumping, corresponding to the scattering of about 100 photons, magnified on two exemplary detuning ranges. Fig. S1(b) is centered around the value used for most of the cooling data presented in the main text.

EXPERIMENTAL DETAILS

The cloud is prepared in a similar way as in Ref. [S6]. Rb atoms are loaded into a MOT from a thermal vapor, followed by a compressed MOT stage where the optical pumping power is strongly reduced, such that the atoms occupy the $F = 1$ ground state manifold. The ODT is turned on at all times and about 1×10^5 atoms are loaded into it when the MOT fields are switched off.

The ODT propagating in the y -direction (see Fig. 1 in the main text), in which the atoms are originally loaded, is focused to a waist of about $10 \mu\text{m}$, while the second ODT propagating in the x -direction has a waist of about $18 \mu\text{m}$ at the position of the atoms. To avoid interference, the beams differ in frequency by 160 MHz. The powers of each trapping beam throughout the sequence are shown in Fig. S2. The (calculated) total trap depths, excluding the influence of gravity but including counter-rotating terms, are $430 \mu\text{K}$ in stage S1 and $14 \mu\text{K}$ in stage X3.

The imaging axis is the same as that of the π beam, which is slightly rotated by $\approx 17^\circ$ from the x -axis in the $x - y$ plane. In Fig. 3(b)-(c), we denote the horizontal axis of the image as y' , which is rotated from the y -axis in the $x - y$ plane by the same angle.

The σ^- optical pumping beam at 795 nm has a highly elliptical shape at the position of the atoms, with waists of $30 \mu\text{m}$ along the x -direction and ~ 1 mm along the y -direction, to optimally address atoms along the sODT. The pumping beam creates a sizable light shift δ_{LS} of the $|2, -1\rangle$ state, given by $\delta_{\text{LS}}/\Gamma_{\text{sc}} = \Delta/\Gamma$, where Γ is the natural linewidth of the $5P_{1/2}$ excited state. Since the state $|2, -2\rangle$ is dark for the σ^- light, there is no appreciable light shift on this state. The light shift is at its largest in stage S1, reaching $\delta_{\text{LS}}/(2\pi) = 500$ kHz. It is determined experimentally by measuring the shift in the Raman resonance. From the measured values of δ_{LS} we deduce the scattering rates Γ_{sc}

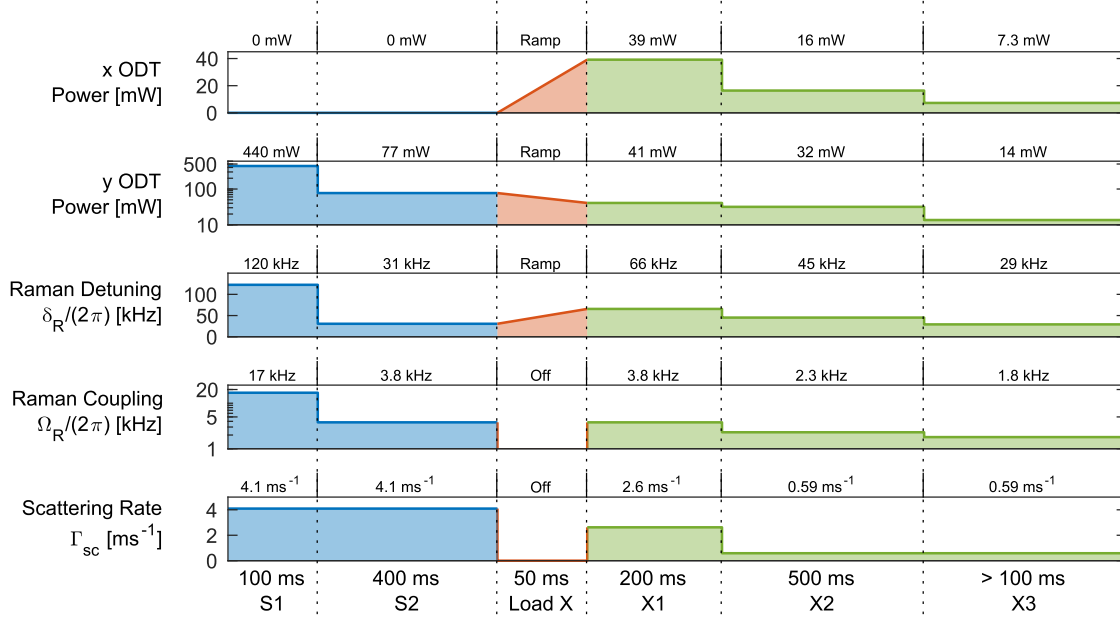


FIG. S2. Optimized multistage Raman cooling sequence. Initially we cool in single beam ODT (blue), then ramp up a second trapping beam (red) to load into a crossed ODT for the final stages of cooling (green).

for $|2, -1\rangle$, shown in Fig. S2. Since the detuning Δ is comparable to the hyperfine splitting of the ground state, the same light also pumps atoms out of the $|5S_{1/2}; F=1\rangle$ manifold.

The π Raman beam propagates in the $x-y$ plane (see Fig. 1 in the main text), with a waist of 0.5 mm. Its light is derived from the same laser that generates the σ^- beam, but it is detuned by 2 MHz from the σ^- using acousto-optic modulators to avoid interference. This makes laser frequency noise common mode between the two beams, thereby loosening the requirements on laser linewidth necessary to have a narrow Raman transition. The Raman beam follows the same path as the light used for absorption imaging, and therefore it is circularly polarized. Over the course of the cooling only its π -polarized component (polarization along the z -axis, i.e. half its power), contributes to the Raman coupling. The other half of the power only adds a negligible amount of scattering and light shift to the $|2, -2\rangle$ state. Very little power ($\lesssim 100 \mu\text{W}$) is required to obtain significant Raman coupling (several kHz, see Fig. S2), so the light shift and scattering rate induced on the $|2, -2\rangle$ state are limited to $\lesssim 0.3$ kHz and $\lesssim 2 \text{ s}^{-1}$, respectively, even at the largest powers used in the cooling sequence.

For all the data presented, each data point is evaluated as an average of 3 to 5 time-of-flight absorption images.

EFFECTIVE RECOIL LIMIT

At trap frequencies in the range 0.1–5 kHz, smaller than the Raman coupling, the cooling operates mostly in the free space limit with unresolved motional sidebands and outside the Lamb-Dicke regime [S7–S9]. Each Raman transition from $|2, -2\rangle$ to $|2, -1\rangle$ transfers $-\hbar\Delta\mathbf{k}$ of momentum to the atoms, where $\Delta\mathbf{k}$ is the difference between the wave vectors of the σ^- and π photons. The kinetic energy removed during one Raman transition for an atom of initial velocity \mathbf{v} is:

$$\begin{aligned} \Delta K_{\text{Raman}} &= \hbar\Delta\mathbf{k} \cdot \mathbf{v} - \frac{\hbar^2|\Delta\mathbf{k}|^2}{2m} \\ &= \hbar\delta_{\mathbf{v}} - 2E_r \end{aligned} \quad (\text{S1})$$

where $\delta_{\mathbf{v}} = \Delta\mathbf{k} \cdot \mathbf{v}$ is the atom's two-photon Doppler shift. The orthogonality of the π and σ^- beams results in $|\Delta\mathbf{k}|^2 = 2|\lambda|^{-2}$, and $E_r = \hbar^2/(2m\lambda^2)$ is the recoil energy of a 795 nm photon. The branching ratio of the optical pumping to the dark state $|2, -2\rangle$ is 1/3, which results in the scattering of an average of 3 σ^- photons to optically pump the atoms following a Raman transition. In the limit of low scattering rate ($\Gamma_{\text{sc}} \ll \omega_{x,y,z}$, which is required to limit reabsorption heating, see below), only the recoil energies of the scattered σ^- photons add, on top of those of

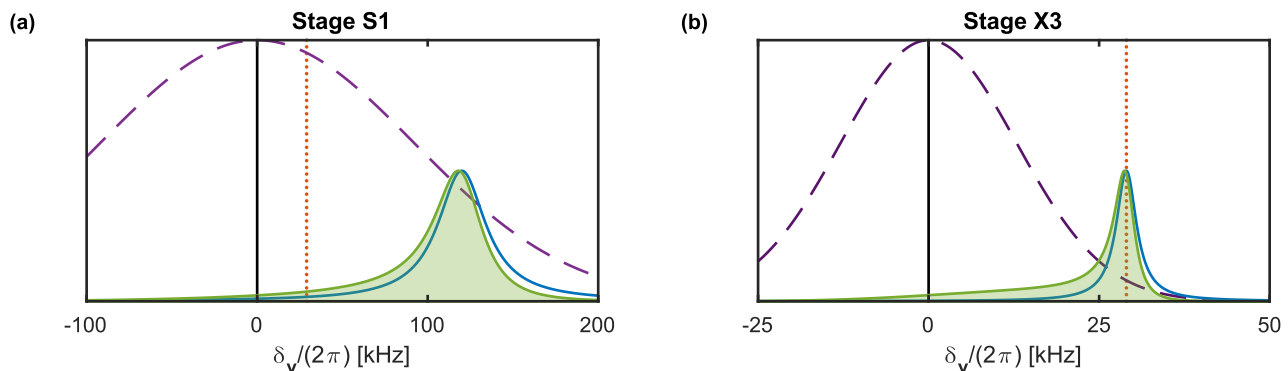


FIG. S3. Thermal velocity distribution (dashed purple), time averaged Lorentzian Raman excitation profile expected given the Raman Rabi frequency (solid blue line), rescaled product of the thermal distribution and the excitation profile (shaded green), and effective recoil limit of 29 kHz (dotted red) for cooling sequence parameters in (a) stage S1 and (b) stage X3. On average, a cooling cycle will cool atoms with velocity greater than the effective recoil limit, and heat atoms with velocity below the effective recoil limit.

the spontaneously emitted photons, resulting in an average net recoil heating of $6E_r$ per optical pumping cycle. The average net energy removed per cooling cycle is then given by:

$$\begin{aligned}\Delta K_{\text{total}} &= \Delta K_{\text{Raman}} - 6E_r \\ &= \hbar\delta_v - 8E_r\end{aligned}\quad (\text{S2})$$

Therefore there is net cooling if and only if the two-photon Doppler shift is larger than $8E_r$, which translates to a kinetic energy in the $\Delta\mathbf{k}$ direction of:

$$K_{\Delta\mathbf{k}} \geq 8E_r = h \times 29 \text{ kHz} \quad (\text{S3})$$

As a result, for temperatures below $T_r^{\text{eff}} = 2.8 \mu\text{K}$ ($\langle K_{\Delta\mathbf{k}} \rangle = \frac{1}{2}k_B T_r^{\text{eff}}$ along $\Delta\mathbf{k}$), the cooling speed drops since only a small fraction of the atoms have Doppler shifts above $8E_r$ where they can be cooled.

OPTIMIZATION OF THE COOLING AND LIMITING FACTORS

For each stage the Raman transitions are tuned to a particular velocity class by adjusting the magnetic field, which differentially shifts the $|2, -2\rangle$ and $|2, -1\rangle$ states. In stage S1, where the mean Doppler shift is much larger than the $8E_r$ limit, we find as expected that the optimal Raman detuning is near the rms Doppler shift, see Fig. S3(a). This is a compromise between removing a large amount of energy per cooling cycle ($\Delta K_{\text{total}} \approx \hbar\delta_R$) and having a sufficiently large probability of finding atoms at those velocities (which drops as δ_R increases). In stage X3 the optimization yields an optimal resonant Doppler shift of $\delta_R/(2\pi) = 29$ kHz. As shown in Fig. S3(b), the probability of finding an atom at these velocities is very small, and the amount of energy removed ΔK_{total} also becomes very small. By averaging ΔK_{Raman} over the actual distribution of addressed atoms [green shaded in Fig. S3(b)] in stage X3, we obtain $\langle \Delta K_{\text{Raman}} \rangle / h = 15$ kHz, well below the recoil heating of $6E_r/h = 22$ kHz, which should lead to heating. Yet cooling is observed, which suggests bosonic enhancement of the branching ratio into the $|2, -2\rangle$ state due to the emerging condensate. A better branching ratio would reduce the average recoil heating during optical pumping, and so cooling could be achieved even when the Raman transition removes less than $6E_r$ of kinetic energy.

At each stage, the strength of the Raman coupling Ω_R is optimized by scanning the power of the π beam. Too small Ω_R lead to a narrow excitation profile, and therefore only a small fraction of the atoms undergo a Raman transition. However, if Ω_R is too large, already “cold” atoms undergo a Raman transition, due to the broadened excitation profile, and are heated during the optical pumping.

Initially in the sODT it is favorable to have a fairly large scattering rate for cooling speed. The smaller number of atoms available to cool in the Boltzmann tail above the recoil energy in the later stages results in a lower optimal scattering rate as it becomes more favorable to decrease reabsorption heating as seen in Fig. 4(c) and discussed below.

For the ODT powers, the main considerations are finding a balance between low density in order to limit inelastic loss and heating, and maintaining large enough trapping frequencies and therefore critical temperatures. Additionally

in the final stage, having a low trap depth has proven crucial to avoid an observed density-dependent heating that increases with trap depth. As pointed out in Ref. [S10], the products of three-body recombination of ^{87}Rb atoms in the $|2, -2\rangle$ state to the least-bound molecular state ($h \times 24$ MHz of binding energy [S11]) can collide with the cold sample before they leave the trap. This was shown to lead to large loss for a collisionally opaque ensemble. In our case, the sample is not collisionally opaque (collision probability ~ 0.1 for s -wave scattering only), nor is the trap deep enough to directly hold recombination products which would dump their energy into the cloud. The presence of a d -wave shape resonance at the energy of the least-bound state for a $^{87}\text{Rb}_2$ molecule is expected to enhance the collisional cross-section of recombination products with the trapped atoms, which could lead to strong losses in the collisionally thick regime. However, we mostly observe heating, which we suspect arises from recombination products undergoing grazing collisions with trapped atoms, with the latter remaining trapped and depositing heat into the cloud. We found that lowering the trap power as much as possible during the final stage X3 to minimize heating was necessary to reach condensation.

The optimized values of the relevant parameters throughout the sequence, namely trap power, Raman detuning δ_R , Raman coupling Ω_R and scattering rate Γ_{sc} , are shown in Fig. S2 for reference.

ESTIMATION OF THE REABSORPTION PROBABILITY

The reabsorption of a scattered photon causes excess recoil heating. This is especially of concern since the reabsorption cross-section, corresponding to a two-photon resonant process, can take on its maximum possible value $\sim 6\pi\lambda^2$. Several strategies have been laid out for suppressing this [S12–S14], boiling down to the use of a low scattering rate Γ_{sc} for optical pumping, a regime known as *festina lente*. With our optimal parameters, we have $\Gamma_{sc} \ll \omega_D, \omega_{x,y,z}$, leading to a suppression of the reabsorption process on the order of Γ_{sc}/ω_D , where ω_D represents the Doppler width. The reabsorption cross-section σ_{reabs} is given by [S13]:

$$\sigma_{\text{reabs}} \approx 4\pi\lambda^2 \frac{\sqrt{\pi}\Gamma_{sc}}{2\sqrt{2}\omega_D} \quad (\text{S4})$$

and the reabsorption probability p_{reabs} is given by:

$$p_{\text{reabs}} \approx \sigma_{\text{reabs}} \langle nl \rangle \quad (\text{S5})$$

where $\langle nl \rangle$ is the mean column density of the cloud. We use the following formula for the mean column density of a thermal cloud, taken from [S10]:

$$\langle nl \rangle = \sqrt{\frac{\pi}{8}} n(0) \sigma_z \frac{\text{artanh}[\sqrt{1 - 1/\varepsilon^2}]}{\sqrt{\varepsilon^2 - 1}} \quad (\text{S6})$$

where $n(0)$ is the peak density, σ_z is the cloud's waist along the short axis of an elongated trap (z -axis here), and $\varepsilon = \omega_y/\omega_z$ is the aspect ratio of the trap. Assuming a classical cloud at the condensation point and a scattering rate $\Gamma_{sc} = 0.59 \text{ ms}^{-1}$, we obtain that a probability for reabsorption $p_{\text{reabs}} \sim 0.1$. Hence reabsorption is not expected to be a significant factor, but it could explain why the performance deteriorates at larger Γ_{sc} in Fig. 4(c) of the main text, since p_{reabs} varies linearly with Γ_{sc} .

* These two authors contributed equally to this work.

† vuletic@mit.edu

- [S1] K. Burnett, P. S. Julienne, and K.-A. Suominen, Laser-Driven Collisions between Atoms in a Bose-Einstein Condensed Gas, *Physical Review Letters* **77**, 1416 (1996).
- [S2] T. W. Hijmans, G. V. Shlyapnikov, and A. L. Burin, Influence of radiative interatomic collisions on dark-state cooling, *Physical Review A* **54**, 4332 (1996).
- [S3] H. Jelassi, B. Viaris de Lesegno, and L. Pruvost, Photoassociation spectroscopy of $^{87}\text{Rb}_2$ ($5s_{1/2} + 5p_{1/2}$) $0g^-$ long-range molecular states: Analysis by Lu-Fano graph and improved LeRoy-Bernstein formula, *Physical Review A* **73**, 032501 (2006).
- [S4] H. Jelassi, B. V. de Lesegno, and L. Pruvost, Photoassociation spectroscopy of $^{87}\text{Rb}_2$ ($5s_{1/2} + 5p_{1/2}$) $0u^+$ long-range molecular states: Coupling with the ($5s_{1/2} + 5p_{3/2}$) $0u^+$ series analyzed using the Lu-Fano approach, *Physical Review A* **74**, 012510 (2006).

- [S5] H. Jelassi and L. Pruvost, Weakly bound $^{87}\text{Rb}_2$ ($5s_{1/2} + 5p_{1/2}$) $1g$ molecules: Hyperfine interaction and LeRoy-Bernstein analysis including linear and nonlinear terms, *Physical Review A* **89**, 032514 (2014).
- [S6] J. Hu, A. Urvoy, Z. Vendeiro, V. Crépel, W. Chen, and V. Vuletić, Creation of a Bose-condensed gas of ^{87}Rb by laser cooling., *Science (New York, N.Y.)* **358**, 1078 (2017).
- [S7] M. Kasevich and S. Chu, Laser cooling below a photon recoil with three-level atoms, *Physical Review Letters* **69**, 1741 (1992).
- [S8] H. J. Lee, C. S. Adams, M. Kasevich, and S. Chu, Raman Cooling of Atoms in an Optical Dipole Trap, *Physical Review Letters* **76**, 2658 (1996).
- [S9] H. Perrin, A. Kuhn, I. Bouchoule, T. Pfau, and C. Salomon, Raman cooling of spin-polarized cesium atoms in a crossed dipole trap, *Europhysics Letters (EPL)* **46**, 141 (1999).
- [S10] J. Schuster, A. Marte, S. Amthage, B. Sang, G. Rempe, and H. C. W. Beijerinck, Avalanches in a Bose-Einstein Condensate, *Physical Review Letters* **87**, 170404 (2001).
- [S11] J. Wolf, M. Deiß, A. Krüchow, E. Tiemann, B. P. Ruzic, Y. Wang, J. P. D’Incao, P. S. Julienne, and J. H. Denschlag, State-to-state chemistry for three-body recombination in an ultracold rubidium gas., *Science (New York, N.Y.)* **358**, 921 (2017).
- [S12] J. I. Cirac, M. Lewenstein, and P. Zoller, Collective laser cooling of trapped atoms, *Europhysics Letters (EPL)* **35**, 647 (1996).
- [S13] Y. Castin, J. I. Cirac, and M. Lewenstein, Reabsorption of Light by Trapped Atoms, *Physical Review Letters* **80**, 5305 (1998).
- [S14] L. Santos, Z. Idziaszek, J. I. Cirac, and M. Lewenstein, Laser-induced condensation of trapped bosonic gases, *Journal of Physics B: Atomic, Molecular and Optical Physics* **33**, 4131 (2000).